Int. J. Electrochem. Sci., 11 **(2016)** 9133 – 9144, doi: 10.20964/2016.11.09

International Journal of ELECTROCHEMICAL SCIENCE
www.electrochemsci.org

Fabrication of a Novel Nickel-Curcumin/Graphene Oxide Nanocomposites for Superior Electrocatalytic Activity toward the Detection of Toxic p-nitrophenol

Sasikumar Ragu[1], *Shen-Ming Chen*[1,*], *Palraj Ranganathan*[2], *Syang-Peng Rwei*[2]

[1] Department of Chemical Engineering and Biotechnology, National Taipei University of Technology, No. 1, Section 3, Chung-Hsiao East Road, Taipei 106, Taiwan, ROC.
[2] Institute of Organic and Polymeric Materials, National Taipei University of Technology, No. 1, Section 3, Chung-Hsiao East Road, Taipei 106, Taiwan, ROC.
[*]E-mail: smchen78@ms15.hinet.net

Received: 23 July 2016 / *Accepted:* 29 August 2016 / *Published:* 10 October 2016

The current study deals with the sensitive electrochemical sensor for ecologically harmful p-Nitrophenol (pNP) based on a glassy carbon electrode which was modified by nickel-curcumin [$Ni(Curc)_2$]/graphene oxide [GO]. The physicochemical properties of the as-prepared nanocomposites were characterized using a different analytical and spectroscopic method, which include UV-Vis spectrophotometer, fourier-transform infra-red spectrophotometer, field emission scanning electron microscopy and cyclic voltammetry. The reduction of pNP at modified GCE revealed linear range 0.49-760 μM, limit of detection 0.016 μM and high sensitivity 0.671μA μM^{-1} cm^2. The recommended sensor was well developed and established the influence of low cost, easily prepare, which is greater to newly reported modified electrodes, thereby permissive practical industrial applications.

Keywords: Electrochemical, Curcumin, p-nitrophenol, Grapheme Oxide, Nickel nitrate, Cyclic voltammetry, Sensor

1. INTRODUCTION

Metal substituted organic compounds have excellent properties in the fields of microbial, biological, cell division, clinical, tumor inhibitor, and insecticidal etc., This is owing to any unemployed coordination sites current on the metal and ligand systems [1]. Curcumin is (1E,6E)-1,7-bis(4-hydroxy-3-methoxyphenyl)-1,6-heptadiene-3,5-dione a yellow color, dyestuff extract from *Curcuma longa* is by eminent well-known due to its unique properties such as antioxidant [2-4], anticancer activities[4,6] and anti-inflammatory properties [6,7].

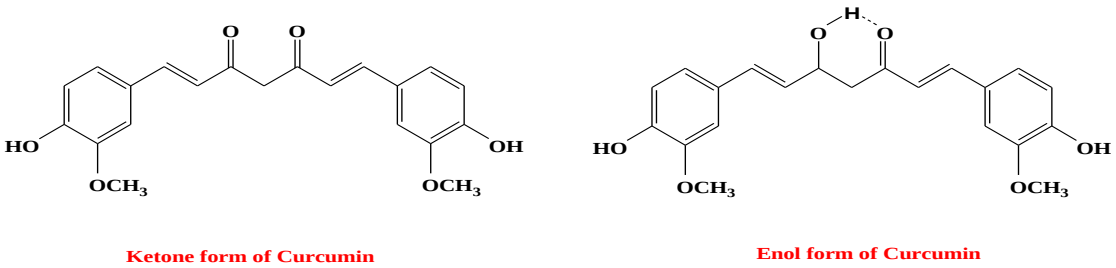

Figure 1. Keto and enol form of curcumin

From the above keto and enol structure of curcumin, it can be has an extremely alternated β-diketone fraction and it is a great natural chelating mediator and its security estimation even managed at high amount in human [8, 9]. After metal complexation of curcumin it has involved very attention more than few years and it is very helpful in the healing of alzheimer's syndrome and in-vitro antioxidant activities. Till now lots of curcumin-metal complexes have been synthesize, characterize and assessed for different genetic behavior [10]. Cu^{2+}-curcumin complex maintain Superoxide Dismutase activity and open radical neutralize ability [11]. Curcumin supported metal complexes have active sites like phenolic and methoxy an enhanced form while the metals occupy a fractional responsibility in additional enlarge its efficacy [12].

Aromatic phenolic nitro compounds, that are commonly used production and synthesis in synthetic and medicine industries such as, artificial dyes, fungicides, pesticides, insecticides, and rubber, are considered environmentally toxicants, which can source irreparable spoil to vegetation and organisms especially little concentrations. When compared to other phenolic derivatives the p-Nitrophenol is more harmful compound [13], that be able to be confirm in agricultural excess and wasterwater, this is due to environmentally degradation of methyl parathion as well as parathion. The injurious personal property of pNP on humans varies depending on exposure time and includes headaches, fever, inhalation trouble and it will cause death at higher levels of dosages [14]. Thus, it is needed to eradicate pNP from polluted wastewater. Comparing pNP with 4-APh gives the product which is less poisonous to neighboring substrate and more eco-friendly in surroundings [15]. Thus, the pNP is removed from the polluted water and it is changed to 4-APh and is used to manufacture of corrosion inhibitors and anticorrosion lubricants [16]. There is a require for the reduction of pNP due to the (aforementioned) significance of 4-APh [17]. So, the reduction of pNP to 4-APh cannot only shrinkage the poisonousness of pNP but also produce an significant industrialized mediator.

In recent decades, many analytical and spectroscopic techniques was developed for sensitive detection of pNP such as GC-EC, HPLC-UV, Spectrophotometric, FSCC-MS/DS, capillary zone electrophoresis and electrochemical analysis in environmental as well as biological samples. Along with them, electrochemical technique has strained significant awareness owing to its tremendous sensitivity and selectivity, quick answer, simple procedure, and price efficiency. Most of the reduction and oxidation studies of pNP have been reported by means of variety of modified electrodes such as glassy carbon electrode (GCE), carbon nanotubes, ordered mesoporous carbons, silver nanoparticles

and poly(methylene blue). However, a greater part of investigate is mainly focused on electrocatalytic action of electrode resources rather than the selectivity and sensitivity of pNP detection [18]

Interestingly, the present study aims to synthesis of [Ni(Curc)2]/GO nanocomposite and the electrochemical reduction of pNP using the above nanocomposite and characterization of synthesized [Ni(Curc)2]/GO nanocomposite by UV-Vis spectrophotometer, FESEM, FTIR and cyclic voltammetry analysis.

2. EXPERIMENTAL SECTION

2.1. Materials

The raw materials for the synthesis of $Ni(Curc)_2$/GO nanocomposite, graphite flakes (~105 mm flakes), potassium permanganate ($KMnO_4$), hydrogen peroxide (H_2O_2), sodium nitrate ($NaNO_3$), hydrochloric acid (10% HCl), p-nitrophenol (pNP), nickel nitrate hexahydrate [$Ni(NO_3)_2.\ 6H_2O$], curcumin ($C_{21}H_{20}O_6$), ethanol (C_2H_5OH) (≥99.8%), were purchased from sigma Aldrich, Taiwan. pH 4.5 of acetate buffer solution was prepared using 0.05 M CH_3COOH and CH_3COONa solutions. All the chemicals were of AR grade and used as received without further purification.

2.2. Methods

2.2.1. Synthesis of graphene oxide

GO was prepared by using the modified Hummers method [19]. In the beginning, graphite flakes (10 g) and $NaNO_3$ (5 g) was added to concentrated sulfuric acid (230 mL) over stirring in a flask wrapped up in an ice-water bath. Then, $KMnO_4$ (30 g) was added gradually, and the mixture was stirred at 30 °C for 2 h. Next, DI water (460 mL) was poured into flask, and the stirred was continued for 30 min at 95 °C. At the end of the reaction, DI water (940 mL) and 5% of H_2O_2 (30 mL) were consequently added to ending the reaction, and the color of the solution twisted yellow from dark brown color. The resulting solid graphene oxide was estranged by centrifugation, washed, and dried under vacuum.

2.2.2. Synthesis of [Ni(Curc)$_2$]/GO nanocomposite

The $Ni(Curc)_2$ complex was synthesis in the following steps. In a typical synthesis a 0.02 mole of curcumin in 10 ml ethanol was added drop wise to 0.01 mole of $Ni(NO_3)_2.6H_2O$ in 10 ml ethanol under stirring. Mean while the mixture pH value was accustomed at 7 by adding a Na_2CO_3 in ethanol solution and stirred at 60 ^{0}C for 4 h until a clear blood-red solution was formed. After that the excess solvent was impassive by under reduced pressure and the residual solid was dried out under vacuum. Finally certain amount of [$Ni(Curc)_2$] was added to GO and ultrasonication for 1 hr to get [$Ni(Curc)_2$]/GO nanocomposite.

2.2.3. Fabrication of $Ni(Curc)_2$ /GO nanocomposite modified electrode

The face of the glassy carbon electrode was with awareness polished to a mirror finish by using a mixture of alumina in water slurry and washed with de-ionized water and it was extra cleaned using water containing ethanol by ultrasonication of the face modified of the electrode. Scheme 1 displays the step-wise preparation of the $Ni(Curc)_2$/GO nanocomposite. The $Ni(Curc)_2$/GO nanocomposite suspension in H_2O was ultrasonicated using a water bath for 1 h. For preparing the $Ni(Curc)_2$ /GO/GCE, the resulting $Ni(Curc)_2$ /GO nanocomposite suspension (8 µL) was drop casted on the surface of the glassy carbon electrode and allowed to dry under hot air oven for 2 h.

2.2.4. Characterization

UV−Vis absorption spectral measurements were recorded with a Jasco V-770 spectrophotometer. Fourier-transform infrared (FT-IR) spectra were recorded using a Bruker IFS28 spectrometer with a spectral resolution of 2 cm^{-1} using dry KBr pellet at ambient temperature. The structure of the sample was examined by field emission scanning electron microscopy (FESEM) at room temperature (25 ºC) using an electron microscopy (JEOL JSM-6500F) that has a field-emission gun with an acceleration voltage at 200 kV. Cyclic voltammetry (CV) and linear sweep voltammetry (LSV) studies were performed using CHI 1205a electrochemical analyzer (CH instruments). A 0.05 M acetate (HAc + NaAc; pH 4.5) buffer solution was act as the supporting electrolyte during the all electrochemical experiments. A conventional three-electrode cell system was utilized using a modified glassy carbon electrode (GCE), Ag/AgCl (saturated KCl), and a platinum wire as the working electrode, reference electrode and counter electrode respectively.

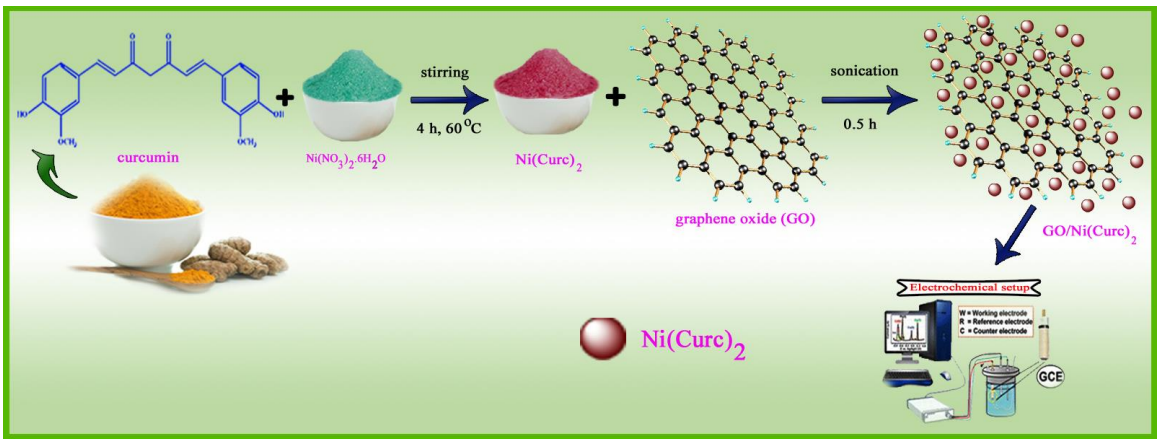

Scheme 1. The detailed synthetic procedure for the formation of $Ni(Curc)_2$/GO nano composite.

3. RESULTS AND DISCUSSION

3.1. UV-Vis analysis of $Ni(Curc)_2$ /GO nanocomposite

In organic solvents like ethanol, acetone, lipids and acetonitrile the curcumin is easily soluble but insoluble in water medium, but the $Ni(Curc)_2$/GO nanocomposite is insoluble in methanol and

acetonitrile but soluble in DMSO only. The comparative electronic UV absorption spectra of Curcumin, GO, $Ni(Curc)_2$ and $GO/Ni(Curc)_2$ in EtOH is shown in Fig 2A. The main absorption band appeared at curcumin due to π-π* shifts at 415-430 nm with compared to GO and the Ni-curcumin complexes displayed the absorption shifted up to 1-8 nm which due to the contribution of carbonyl group in curcumin after complexation with metals. Owing to a curcumin (L) ⟶ metal (M^{n+}) ion the shoulders appeared at 418-423 nm. The UV spectrum of the GO, $Ni(Curc)_2$/GO nanocomposite showed the absorbance maximum at 230, 232 nm and shoulders appear at 295 nm respective corresponds to the electronic dipole permitted π-π* kind excitation. The spectral detail has been summarized in Table 1. [20].

3.2. FTIR analysis of $Ni(Curc)_2$ /GO nanocomposite

Fig. 2B and Table 2 revealed FTIR spectrum in curcumin the phenolic O-H stretching frequency appeared at 3506 cm^{-1} with very sharp peak and ν(OH) group (in enol form) stretching band appeared at a range between 3200-3500 cm^{-1} with broad band, which is due to the ν(OH) group (in enol form). The aromatic ν(C-H) frequency appeared at 3079 – 3000 cm^{-1} with lower intensities. The stretching vibrations of ν(C=C) and ν(C=O) in curcumin appeared at 1274 and 1429 cm^{-1}. The significant characteristic of solid state FTIR spectra of the nanocomposite exhibited by the occurrence of O-H stretching, C-H stretching, C=O stretching, C=C stretching, C-O stretching in OCH_3 and phenol, and C-H stretching in aromatic. In nanocomposite the bands appeared at 1512, 1385 cm^{-1} due to C=O stretching C=C stretching respectively ought to be shifted to lower frequencies while complexation. IR spectrum of ligand curcumin showed ν(C=O) at 1429 cm^{-1} and ν(C=C) at 1274 cm^{-1}, shifted to lower energy in the metal nanocomposite of the same ligand. The water molecule frequency presence at 3200-3600 cm^{-1} with broad band. This is confirmed that the ligand coordinates with the central metal ions through the C=O group. The formation of M-O bond was confirmed by the presence of new bands occurred at 496-505 cm^{-1} [21, 22].

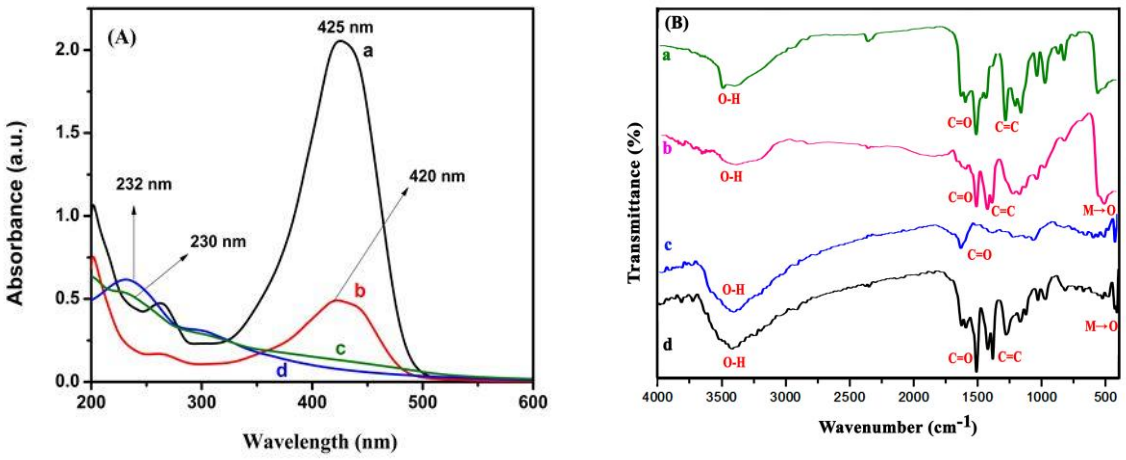

Figure 2. (A) UV - Vis spectra (B) IR spectra of (a) Curcumin (b) $Ni(Curc)_2$ (c) GO (d) $Ni(Curc)_2$ /GO

Table 1. UV-Vis Spectrum details of curcumin and its nanocomposite in EtOH

Compound	**UV-Vis peaks (in nm)**		
Curcumin	425 (λ_{max})	-	262
GO	230 (λ_{max})	295	-
Ni(Curc)$_2$	420 (λ_{max})	-	263
Ni(Curc)$_2$/GO	232 (λ_{max})	295	-

Table 2. FTIR spectrum details of curcumin and its nanocomposite

Compound	**FTIR (in cm^{-1})**			
	ν (O-H)	**ν (C=O)**	**ν (C=C)**	**ν (M-O)**
Curcumin	3506, 3200-3600	1429	1274	-
GO	3420, 3200-3600	1730	1622	-
Ni(Curc)$_2$	3411,3200-3600	1422	1269	496
Ni(Curc)$_2$/GO	3425, 3200-3600	1512	1385	-

3.3. FESEM analysis of Ni(Curc)$_2$ /GO nanocomposite

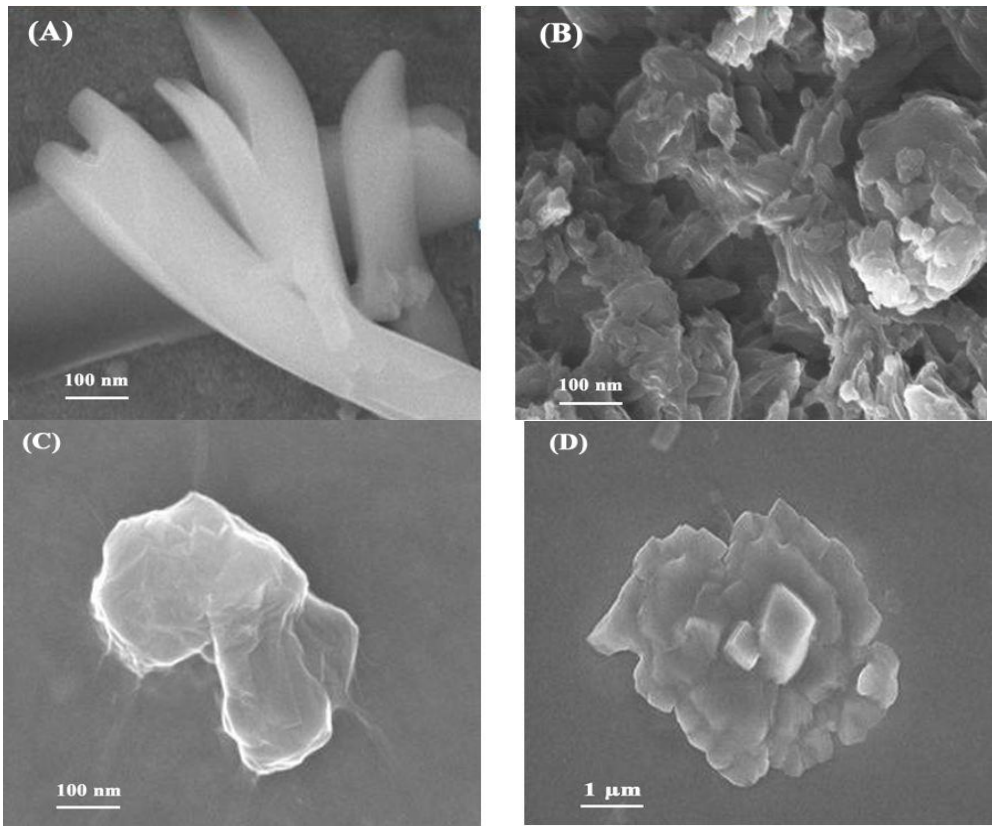

Figure 3. FESEM images of (A) Curcumin (B) Ni(Curc)$_2$ (C) GO (D) Ni(Curc)$_2$ /GO nanocomposite

The surface morphology of curcumin, Ni(Curc)$_2$, GO and Ni(Curc)$_2$/GO nanocomposite was analyzed by field emission scanning electron microscope (FESEM) with different magnification and

the micrographs are displayed in Fig. 3A-D. FESEM (Fig. 3D) of $Ni(Curc)_2$ /GO nanocomposite shows the characteristic morphology of GO along with decoration of $Ni(Curc)_2$ nanocomposite with size ranging in nanometers. The FESEM micrograph represents the nano-granular morphology created by the aggregation of little globular structures. The particles nature is asymmetrical in structure with amorphous morphology and some of particles in agglomeration nature.

3.4. Electrochemical behavior of pNP at $Ni(Curc)_2$ /GO nanocomposite modified electrode

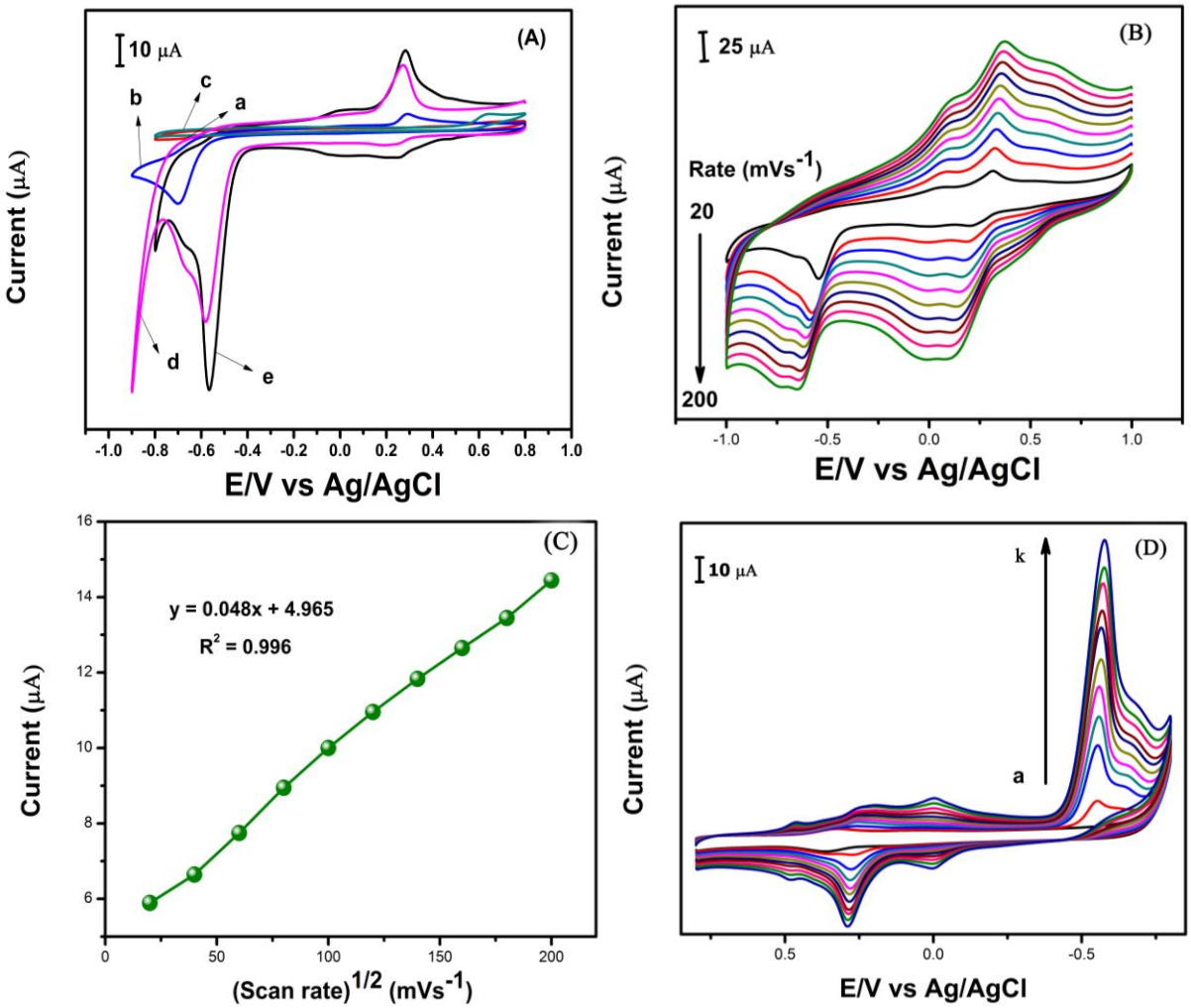

Figure 4. (A) Electrochemical performance of 3×10^{-4} M pNP at (a) $Ni(Curc)_2$/GO nanocomposite modified GCE absence of pNP (b) bare GCE presence of pNP, (c) curcumin, (d) GO, (e) $Ni(Curc)_2$/GO nanocomposite modified GCE presence pNP were investigated in 0.05 M acetate (HAc + NaAc; pH 4.5) buffer solution. (B) Cyclic voltammograms of $Ni(Curc)_2$/GO nanocomposite modified GCE in deoxygenated acetate buffer at different scan rates (20–200 mV s^{-1}). (C) Plot of v1/2 vs. I_p. (D) Cyclic voltammograms obtained at $Ni(Curc)_2$/GO nanocomposite modified GCE in 0.05 M acetate (HAc + NaAc; pH 4.5) buffer solution in the absence (a) and presence of every addition of 1 µM pNP (curves b to j) at the scan rate of 50 mVs^{-1}.

3.5. Electrocatalysis of pNP at Ni(Curc)$_2$/GO nanocomposite modified GCE

To assess the electrocatalytic activity of the various modified and unmodified electrodes was examined by CVs. Fig. 4A presents the cyclic voltammogram curves of 100 μM pNP in 0.05 M of pH 4.5 acetate buffer solutionat various electrodes such as, (a) Ni(Curc)$_2$/GO nanocomposite modified GCE absence of pNP (b) bare GCE presence of pNP, (c) curcumin, (d) GO, (e) Ni(Curc)$_2$/GO nanocomposite modified GCE presence pNP in acetate buffer solution (pH 4.5) containing 10 mM of pNP at the scan rate of 50 mV s^{-1}**.** The electrocatalytic activity is follows the order: curcumin<GCE<GO< Ni(Curc)$_2$/GO nanocomposite modified GCE.

Due to poor electrocatalytic ability of curcumin there is no reduction peak with quantifiable peak currents. There is no reduction peak appeared when introduced into electrochemical setup modified GCE without pNP. The addition of pNP in bare GCE shows little bit variation in the CV curve with a small peak current (-0.69 V) at E_{pc} (reduction peak potential) with small current. Moreover, a remarkable signal was observed at -0.58 V and -0.56 V for the pure graphene oxide and Ni(Curc)$_2$/GO nanocomposite modified GCE. The well defined redox peak and significant reduction peak potential (E_{pc}) and oxidation peak potential (E_{pa}) were observed at -0.56 and 0.28 V for the Ni(Curc)$_2$/GO nanocomposite modified GCE. The sharp peak appeared at -0.56 V with high peak current exhibits at Ni(Curc)$_2$/GO modified GCE, as shown in Fig. 4A. From the above results it is concluded that the electrochemical detection of pNP is a reversible two electron transfer reduction-reduction process [23-25]. Scheme 2 shows the [26,27,28], the redox mechanism of pNP. However comparatively, Ni(Curc)$_2$/GO nanocomposite modified GCE is showed maximum electrocatalytic performance compared to GO in terms of high peak currents and less over potential. Thus, Ni(Curc)$_2$/GO nanocomposite modified GCE has superior electrocatalytic ability to the reduction of pNP due to perfect synergy between high conductivity and large surface area of the GO and excellent electrocatalytic ability of Ni(Curc)$_2$.

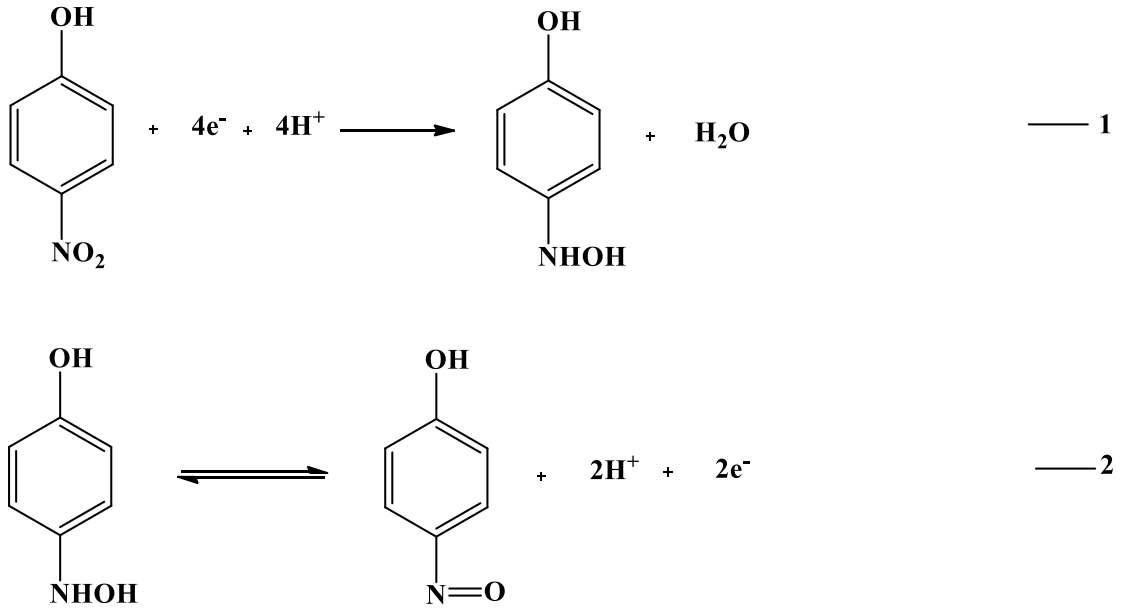

Scheme 2. Mechanism about electrochemical detection of pNP

The huge reduction peaks happen at peak potentials of -0.56 and 0.28 V due to $4e^-/4H^+$ reduction of the pNP to p-(hydroxyamino) phenol, and the redox effect in high potential region originate from the oxidation of p-(hydroxyamino) phenol to p-nitrosophenol [29]. The pNP molecules was absorbed by the modified electrodes and are reduced at -0.56 V. The CV curves obviously confirms that the $Ni(Curc)_2$/GO nanocomposite modified GCE is a good electrochemical detection of pNP.

3.6. Different scan rates

Fig. 4B is a scan rate on electrocatalytic activity of $Ni(Curc)_2$/GO nanocomposite modified GCE for the detection of pNP is further exemplified by the $Ni(Curc)_2$/GO nanocomposite. The CV curves obviously explain constant increases in the anodic and cathodic peak currents when increasing the scan rates series from 20 to 200 mV s^{-1}. In addition, a plot among square root of the scan rates (ν1/2) versus reduction peak current has exhibit a linear relationship which demonstrating that the reduction process of pNP occurring at the $Ni(Curc)_2$/GO nanocomposite modified glassy carbon electrode is a diffusion controlled electron transfer process (Fig. 4C). From the results we confirm that the witnessed CV responses are due to the detection of pNP molecules diffused on the surface of the $Ni(Curc)_2$/GO nanocomposite modified GCE. The inset in Fig. 4B displays the plot between cathodic peak current and the square root of scan rate, which may be expressed by a linear regression equation as E_{pa} (V) = 0.048x + 4.965, R^2 = 0.996. All these results clearly confirm that the process is a diffusion controlled reversible process [26,27,28].

Fig. 4D shows the CV curves for the detection of pNP with various concentration obtained at $Ni(Curc)_2$/GO nanocomposite modified GCE in pH 4.5 acetate buffer solution in the presence of pNP (curves b to k; every addition of 1 µM concentration of pNP and absence (curve a). The cathodic peak current is increases with increase in every additions of pNP. The inset in Fig 4D corresponds to the electrochemical curve, which shows the linear dependence of peak current (I_{pc}) with the different pNP concentrations. Additionally, the potential shift of the peak currents in not affected by increasing pNP concentration. The limit of detection is calculated using the below equation.

$$LOD = 3S_b/b \qquad \text{------- 3}$$

The limit of detection is calculated by using the slope of the straight line of the electrochemical analytical curve and SD of the mean value for ten voltammograms of the blank ($\mathbf{S_b}$). [29,30] The $Ni(Curc)_2$/GO nanocomposite modified GCE based sensor showed very fast and sensitive responses for the every addition of pNP.

3.7. Deterrmination of p-nitrophenol

The determination of pNP over $Ni(Curc)_2$/GO modified GCE were investigated by LSV measurements. Fig 5 shows that LSV curves of pNP for different concentrations of the $Ni(Curc)_2$/GO modified GCE at 50 mV s^{-1}. The cathodic peak current happens at a -0.56 V, parallel to the reduction of pNP. The cathodic peak currents increase linearly with increasing concentrations in the range from

0.49 to 760 µM (inset) with detection limit 0.016 µM and sensitivity of 0.671µA µM-1 cm^2. From these above results revealed that the $Ni(Curc)_2$/GO nanocomposite modified GCE have specific electrocatalytic activity against pNP, which is the major explanation for the successful electrochemical detection.

Table 3 will explain the similarity of analytical parameters like as, limit of detection, sensitivity and concentration range for the various modified GCE occupied in the detection of pNP.

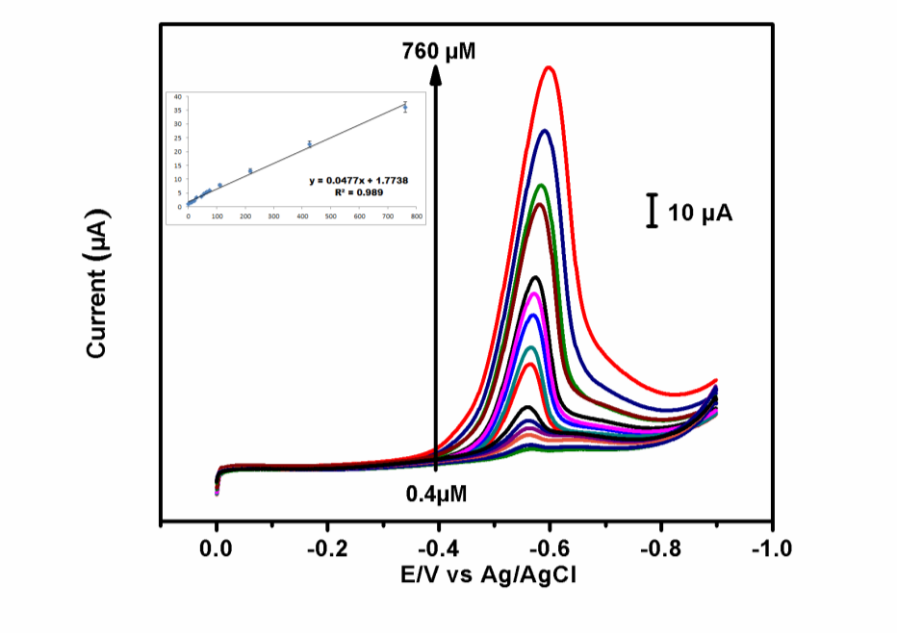

Figure 5. LSV curves of $Ni(Curc)_2$/GO nanocomposite modified GCE under varied pNP concentrations (curves a-p) in 0.05 M acetate (HAc + NaAc; pH 4.5) buffer solution recorded at scan rate of 50 mV s^{-1} .

Table 3. Similarity of analytical parameters for detection of pNP at a variety of modified GCE

Electrode Substrate	Concentration range (µM)	Limit of detection (µM)	Sensitivity (µA $µM^{-1}$ cm^{-2})	Reference
Multiwalled Carbon nanotube/Polydiphenyl amine/glassy carbon electrode	8.9-1500	-	0.632	30
Au nanoparticles/glassy carbon electrode	10-1000	8.0	-	31
Nano Cu_2O/glassy carbon electrode	1-400	0.5	-	32
Ag nanoparticles/glassy carbon electrode	0.1-350	0.015	2.570	33
Graphene-Au nanoparticles/glassy carbon electrode	0.47-10750	0.47	0.053	34
Activated carbon/glassy carbon electrode	1-500	0.16	5.810	29
Graphene/nafion/screen printed carbon electrode	10-620	0.6	-	35
Ag nanoparticles/glassy carbon electrodes	1.5-140	0.5	0.043	36
6,7,9,10,17,18,19,20,21,22-decahydrodi benzo [h,r][1,4,7,11,15] trioxadiazacyclonanodecine-16,23-dione/Carbon paste electrode	1-100	0.25	-	37
Hydroxylapatite nanopowder	1-300	0.6	-	38
Nickel-curcumin/graphene oxide nanocomposite/glassy carbon electrode	0.49-760	0.016	0.671	This work

4. CONCLUSIONS

In conclusion, we have effectively made-up a $Ni(Curc)_2$/GO nanocomposite film by a simple *In-situ* method. The assemble nanocomposite film was characterized by field emission scanning electron microscopy, which revealed that the nano-granular structure. The synthesized nanocomposite has high dispersible property in different solvents such as ethanol, water, N-methyl-2-pyrrolidone and Dimethyl formamide. The modified GCE of $Ni(Curc)_2$ nanocomposite have superior electrocatalytic activity towards the detection of pNP. The electrochemical behavior of the $Ni(Curc)_2$/GO nanocomposite film were examined using cyclic voltammetry and linear sweep voltammetry (LSV). The nanocomposite adapted GCE has a highly electro active surface area, that is well matched to the voltammetric finding of pNP. The assembled sensor exhibits a tremendous electrocatalytic performance with a low limit of detection and good sensitivity property.

References

1. F.A. Cotton and G. Wilkinson, Advanced Inorganic Chemistry: A Comprehensive Text, Interscience Publishers, New York (1966).
2. M. Sreejayan and N. A. Rao, *J. Pharm. Pharmacol.* 46 (1994) 1013. http://dx.doi.org/10.1111/j.2042-7158.1994.tb03258.x
3. M. K. Unnikrishnan and M. N. A. Rao, *Pharmazie* 50 (1995) 490.
4. H. P. T. Ammon and M. A. Wahl, *Pharm. Curcuma longa Planta Med*. 57 (1991) 1. http://dx.doi.org/10.1055/s-2006-960004
5. R. J. Anto, G. Kuttan, K. V. D. Babu, K. N. Rajasekharan, and R. Kuttan, *Int. J. Pharm*, 131 (1996) 1. http://dx.doi.org/10.1016/0378-5173(95)04254-7.
6. V. Anto, G. Kuttan, K. V. D. Babu, K. N. Rajasekharan, and R. Kuttan, *Pharm. Pharmacol. Commun.* 4 (1998) 103.
7. H. H. Tønnesen, H. D. Vries, J. Karlsen, and G. B. Van, *J. Pharm. Sci*. 76 (1987) 371. http://dx.doi.org/10.1002/jps.2600760506.
8. T.M. Kolev, E.A. Velcheva, B. A. Stamboliyska, and M. Spiteller, *Int. J. Quant. Chem*. 102 (2005, 1069. http://dx.doi.org/10.1002/qua.20469.
9. B. Zebib, Z. Mouloungui, and V. Noirot, *Bioinorg. Chem. Appl*. 1 (2010). http://dx.doi.org/10.1155/2010/292760.
10. M.A. Subhan, Y. Hasegawa, T. Suzuki, S. Kaizaki, and Y. Shozo. *Inorg. Chim. Acta* 362 (2009) 136. http://dx.doi.org/10.1016/j.ica.2008.03.093.
11. Atanu Barika, Beena Mishraa, Liang Shenb, Hari Mohana, R.M. Kadamc, S. Duttad, Hong-Yu Zhangb, K. Indira Priyadarsinia. *Free Radical Biology & Medicine*. 39 (2005) 811. doi:10.1016/j.freeradbiomed.2005.05.005.
12. Haroon Khalid Syed, Muhammad Adnan Iqbal, A. Rosenani Haque & KokKhiang Peh. 68 (2015) 1088. http://dx.doi.org/10.1080/00958972.2014.1003051.
13. S. Raja, V. Ramesh, V. Thivaharan, *J. Ind. Eng. Chem*. 27 (2015) 59.
14. A. Saravanakumar, M. Ganesh, J. Jayaprakash, H. Jang, *J. Ind. Eng. Chem*. 28 (2015) 277.
15. K.J.P. Anthony, M. Murugan, M. Jeyaraj, N.K. Rathinam, G. Sangiliyandi, *J. Ind. Eng. Chem*. 20 (2014) 2325.
16. K. Ramachandran, D. Kalpana, Y. Sathishkumar, Y.S. Lee, K. Ravichandran, G. Gnana kumar, *J. Ind. Eng. Chem.* 35 (2016) 29.
17. S.S. Li, D. Du, J. Huang, H.Y. Tu, Y.Q. Yang, A.D. Zhang, *Analyst.* 138 (2013) 2761.

18. G. D. Christian and J. E. O'Reilly. Ultraviolet and Visible Absorption Spectroscopy in Instrumental Analysis, 2nd edition (Allyn and Bacon Publisher, Boston, 1986.
19. B. Paulchamy, G. Arthi and B.D. Lignesh, *J Nanomed Nanotechnol*. 6 (2015) 1. http://dx.doi.org/10.4172/2157-7439.1000253.
20. Veerappan Mani, Rajkumar Devasenathipathy, Shen-Ming Chen, Karuppasamy Kohilarani, Rasu Ramachandran, *Int. J. Electrochem. Sci*., 10 (2015) 1199.
21. X. -Z. Zhao, T. Jiang, L. Wang, H. Yang, S. Zhang, and P. Zhou, *J. Mol. Struct*. 984 (2010) 316. http://dx.doi.org/10.1016/j.molstruc.2010.09.049.
22. K. Mohammadi, K. H. Thompson, B. O. Patrick, T. Storr, C. Martins, E. Polishchuk, V. G. Yuen, J. H. McNeill, and C. Orvig, *J. Inorg. Biochem*. 99 (2005) 2217. http://dx.doi.org/10.1016/j.jinorgbio.2005.08.001.
23. L. Luo, X. Zuo, Y. Ding and Q. Wu, *Sens. Actuators*, B. 135 (2008) 61.
24. F. C. Moraes, S.T. Tanimoto, G.R.S. Banda, S.A.S. Machado and L.H. Mascaro, *Electroanalysis*. 21 (2009) 1091.
25. M.A. Mhammedi, M. Achak, M. Bakasse and A. Shtaini, *J. Hazard. Mate*r., 163 (2009) 323.
26. S. Hu, C. Xu, G. Wang, D. Cui, *Talanta* 54 (2001) 115.
27. M. Mhammedi, M. Achak, M. Bakasse, A. Chtaini, *J. Hazard. Mater*. 163 (2009) 323.
28. M. Li, H. Wu, J. Hu, C. Ma, *Acta Phys. Chim. Sin.* 24 (2008) 1937.
29. R. Madhu, C. Karuppiah, S.-M. Chen, P. Veerakumar, S.-B. Liu, *Anal. Methods*, 6 (2014) 5274.
30. Y.-L. Yang, B. Unnikrishnan, S.-M. Chen, *Int.J. Electrochem. Sci.*, 6 (2011) 3902.
31. L. Chu, L. Han and X. Zhang, *J. Appl. Electrochem*., 41 (2011) 687.
32. H. Yin, Y. Zhou, S. Ai, Q. Ma, L. Zhu and L. Lu, *Int. J. Environ. Anal. Chem.*, 92 (2012) 742.
33. C. Karuppiah, S. Palanisamy, S. M. Chen, R. Emmanuel, M. A. Ali, P. Muthukrishnan, P. Prakash and F. M. A. Al- Hemaid, *J. Solid State Electrochem.*, 18 (2014) 1847.
34. W. Zhang, J. Chang, J. Chen, F. Xu, F. Wang, K. Jiang and Z. Gao, *Res. Chem. Intermed.*, 38 (2012) 2443.
35. A. Arvinte, M. Mahosenaho, M. Pinteala, A. M. Sesay and V. Virtanen, *Microchim. Acta*, 174 (2011) 337.
36. I. G. Casella and M. Contursi, *J. Electrochem. Soc.*, 154 (2007) 697.
37. G. Rounaghi, R. M. Kakhki and H. Azizi-toupkanloo, *Mater. Sci. Eng., C*, 32 (2012) 172.
38. H. Yin, Y. Zhou, S. Ai, X. Liu, L. Zhu and L. Lu, *Microchim. Acta*, 169 (2010) 87.